Transforming information from spin encoding to route encoding

Aiping Liu (刘爱萍)[1,2], **Xiao Xiong (熊　霄)**[1,2], **Xifeng Ren (任希锋)**[1,2*], **and Guangcan Guo (郭光灿)**[1,2]

[1]*Key Laboratory of Quantum Information, University of Science and Technology of China, Hefei 230026, China*

[2]*Synergetic Innovation Center of Quantum Information & Quantum Physics, University of Science and*
Technology of China, Hefei 230026, China

Corresponding author: renxf@ustc.edu.cn

Spin (polarization) is widely used in free-space optics, while in photonic integrated circuits (PICs), information is usually encoded in optical route. So a practical way to connect these two encoding methods is necessary for information communication. In this letter, an encoding convertor is designed to connect spin encoding and route encoding. Finite element method is used to calculate the conversion efficiency and extinction ratio of the encoding convertor and the theoretical analyses are also given. Our protocol shows a friendly way to convert optical spin information to route information, which will promote the compatibility of free-space optics and PICs.

OCIS codes: 240.6680, 250.5300, 230.5440.

doi: 10.3788/COL201412.072401.

Surface plasmon polariton (SPP), i.e., the collective oscillation of electrons in the metal-dielectric interface, has been widely studied, since its unique properties are highlighted in the extraordinary transmission phenomenon[1]. SPP is able to carry on the optical spin angular momentum and orbital angular momentum of photon, which can be used to encode information in quantum communication[2−4]. And thanks to its free ness of diffraction limit, photonic integrated circuits (PICs) are merged to a more integrated scale by employing SPP as an information carrier[5,6]. What is more, since the properties of SPP are polarization-dependent, the propagating route of SPP is manipulable by engineering the metal structure and incident polarization, which makes it more popular in the applications of PICs[7−9].

In PICs, since the operations are challenging, a proper method to encode information is especially important[10,11]. Compared with other encoding ways, route encoding has its own advantages in PICs[12−15]. However, in free-space optics, the information is usually encoded in optical spin state, which is challenging to be realized in PICs. Thus, an encoding convertor from spin encoding to route encoding becomes necessary for the interconnection between free-space optical circuits and PICs.

Here, we demonstrate a method to convert spin encoding to route encoding based on the polarization-dependent excitation of SPP. A device called encoding convertor is designed, with an input port composed of rectangle groove arrays and two output ports connected with two waveguides (SPP propagating routes for encoding information). By elaborately designing the groove arrays in the input area, the encoding convertor can couple photons in different spin states to SPP propagating in different waveguides, which realizes the conversion from spin encoding to route encoding.

The designed encoding convertor is a rhombus structure with an input port in the center and output ports on two sides, as illustrated in Fig. 1(a). In the input port, there are four arrays and each array contains 4, 5, 5, 4 units, which includes two rectangle grooves with tilted

angles of θ_1 and θ_2, as shown in the inset of Fig. 1(b). We take $\theta_1 = 45°$ and $\theta_2 = -45°$ to make sure that the SPP excited by the right-handed and left-handed circular polarizations, which are the spin eigenstates of photons, can be coupled to the right and left waveguides[16]. In order to match the momentum mismatch between excitation light and SPP, the other geometric parameters of the convertor are selected as $w = 25$ nm, $t = 110$ nm, $S = 105$ nm, $L_c = 3.0$ μm, $\varphi = 30°$, and $L_w = 1$ μm, respectively. And each output port of the convertor is connected with a waveguide, to which the encoded SPPs flow. The encoding convertor is made of Polymethyl Methacrylate (PMMA), which is deposited on a 200-nm-thick gold film on the SiO$_2$ substrate. The rectangle grooves are etched through 160-nm-deep PMMA and extend into the gold film for 100 nm. The intensity distribution of SPPs on the encoding convertor is calculated by finite element method (COMSOL Multiphysics 4.2). In the calculation, we take the permittivities of gold as $\varepsilon_m = -11.96 + 1.13i$ and PMMA as $\varepsilon_d = 2.23$ corresponding to the vacuum wavelength of 670 nm[17]. And the refractive indices of air and SiO$_2$ are 1 and 1.5, respectively.

The intensity distributions of SPPs under different excitation conditions are illustrated in Figs. 1(c)–(f). In Figs. 1(c) and (d), SPPs excited by photons in right-handed and left-handed circular polarizations (shown by the white arrows) are coupled into the right and left waveguides, respectively. In the waveguide, SPPs propagate as fundamental mode, whose intensity distribution in the cross-section along the white dashed cutting line is illustrated in the inset of Fig. 1(c). And in the cases of linear polarization excitations (Figs. 1(e) and (f)), the excited SPPs are coupled to both waveguides, since the linear polarization is the superposition of right-handed and left-handed circular polarizations. These results demonstrate that different spin states of photon can be converted to different propagation routes of SPPs. In the following, theoretical analyses are given to explain the above phenomena.
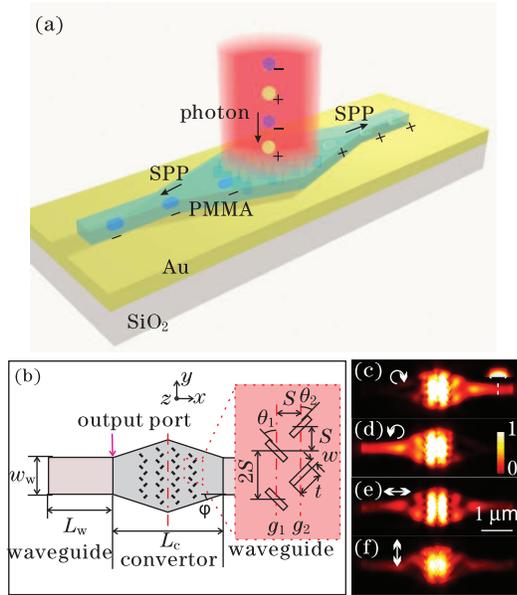
Fig. 1. (a) Diagram of the encoding convertor with light incident on it. Yellow balls and purple balls denote the photons in the spin states of $|+\rangle$ and $|-\rangle$. Capsules denote SPPs. (b) Illustration of the encoding convertor. (c)–(f) give the intensity distributions of SPPs excited with right-handed circular, left-handed circular, x linear and y linear polarizations, respectively.

To describe the state of the incident light, we denote the spin states of right-handed and left-handed circular polarizations as $|+\rangle$ and $|-\rangle$, which constitute a set of complete orthogonal state bases. Then, an arbitrary spin state can be given as $|\Psi\rangle = \phi|+\rangle + \exp(i\Delta)\sin\phi|-\rangle$, where $\cos\phi$ and $\sin\phi$ are the amplitudes of $|+\rangle$ and $|-\rangle$, and Δ is the phase difference between $|+\rangle$ and $|-\rangle$. As shown in Fig. 1(b), light in different spin states is incident on the encoding convertor and SPP is excited on the groove arrays where the momentum matching condition is satisfied. The excited SPP propagates along the interface between gold and PMMA with a wave vector $k_{\mathrm{SPP}} = k_0[\varepsilon_{\mathrm{m}}\varepsilon_{\mathrm{d}}/(\varepsilon_{\mathrm{m}} + \varepsilon_{\mathrm{d}})]^{1/2}$. Establishing the coordinate system shown in Fig. 1(a), SPPs along the y-direction interfere destructively resulting in a zero propagation vector, since the structure is specially designed. Therefore, this part of SPPs is out of consideration in the following analyses. For simplicity, a pair of grooves is considered and the centers of grooves 1 and 2 are at points $x = 0$ and $x = S$. With an incident light in the spin state $|\Psi\rangle$, the excited SPPs can be expressed as[18]

$$|\psi_1\rangle = C_1^{1/2}[\cos\phi + \exp(i\Delta)\sin\phi]\exp(-k_z z)\times$$
$$\{\exp[i(k_x x - \omega t)]|R\rangle + \exp[-i(k_x x + \omega t)]|L\rangle\}, \quad (1)$$

$$|\psi_2\rangle = C_2^{1/2}\{\exp(-i\delta)\cos\phi + \exp[i(\delta + \Delta)]\sin\phi\}\times$$
$$\exp(-k_z z)\{\exp\{ik_x(x - S) - i\omega t\}|R\rangle +$$
$$\exp[-ik_x(x - S) - i\omega t]|L\rangle\}, \quad (2)$$

where C_1 and C_2 are the excitation efficiencies, k_z and k_x are z and x components of $k_{\mathrm{SPP}} = (k_x^2 + k_z^2)^{1/2}$, and δ is the phase difference determined by $\delta = \theta_1 - \theta_2$. $|R\rangle$ and $|L\rangle$ are the states of SPPs propagating along the right and left waveguides, respectively. Then SPPs propagat-

ing in the two waveguides are given as the superposition function $|\psi\rangle = |\psi_1\rangle + |\psi_2\rangle$. Considering the absorption loss in metal, the wave vector of SPP can be expressed as a complex form $k_{\mathrm{SPP}} = \beta + i\gamma$, with β and γ being its propagation vector and propagation loss factor. Considering that the distance between grooves 1 and 2 is 105 nm and $\gamma = 0.00017~\mathrm{nm}^{-1}$, it is reasonable to take $\gamma S \approx 0$. Besides, we have $\delta = \pi/2$ and $\beta S = \pi/2$. Taking $C_1 = C_2 = C$ for simplicity, the probability of SPPs coupled to the right waveguide can be given as

$$P_{\mathrm{R}} \approx \cos^2\phi \int_{s_o} 2\widetilde{C}_1 \mathrm{d}s, \quad (3)$$

and the probability of SPPs reaching the left waveguide is

$$P_{\mathrm{L}} \approx \sin^2\phi \int_{s_o} 2\widetilde{C}_2 \mathrm{d}s, \quad (4)$$

where $\widetilde{C}_j = \rho_j C$ ($j = 1, 2$), ρ_j is the effective efficiency of SPP coupled to the waveguides, s_o is the cross section of the output ports of the encoding convertor. Equations (3) and (4) illustrate that the probabilities of SPPs coupled to the right and left waveguides are proportional to the probabilities of $|+\rangle$ and $|-\rangle$, respectively. This means that the information encoded in optical spin states is transformed to that encoded in different route states of SPPs.

Figure 2(a) gives the probabilities of SPPs coupled to the waveguides, in other words, the conversion efficiency of the encoding convertor, as a function of ϕ. Here, the black (red) line denotes the SPPs flowing to the right (left) waveguides. According to Eqs. (3) and (4), the probabilities of SPPs coupled to each waveguide vary as trigonometric function with a period of π, which agrees well with the numerical results shown in Fig. 2(a). For $\phi = 0$, corresponding to the right-handed polarization excitation, the probability of SPP coupled to the right waveguide is maximum while that to the left waveguide reaches minimum. In the case of $\phi = \pi/2$ (left-handed circular polarization), it is opposite to the former one that the probability of SPP coupled to the right waveguide reaches minimum and that to the left one reaches maximum. That is to say, the probabilities of SPPs coupled to the two waveguides sinusoidally oscillate with a phase difference of $\pi/2$.

In addition to the conversion efficiency of the encoding convertor, the extinction ratio which is defined as the ratio of SPPs coupled to the two waveguides, is given in Fig. 2(b). The maximum extinction ratio reaches $93:1$ for $P_{\mathrm{L}}:P_{\mathrm{R}}$ and $76:1$ for $P_{\mathrm{R}}:P_{\mathrm{L}}$ at the frequency of 447 THz, which makes the convertor feasible in the information transmission. A high extinction ratio promises
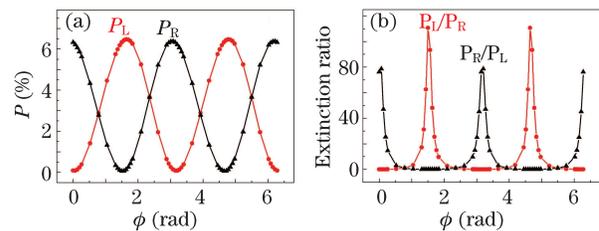

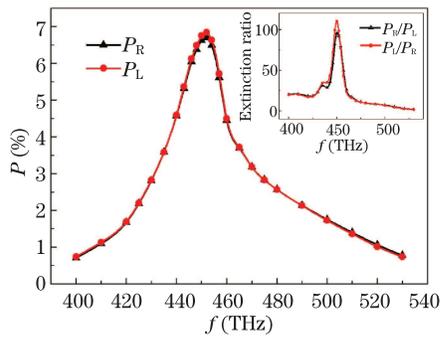Fig. 2. (a) Conversion efficiency and (b) extinction ratios of the encoding convertor.

Fig. 3. Conversion efficiency of the encoding convertor. The inset gives the corresponding extinction ratios.

the discrimination of different eigenstates with high accuracy and reduces the bit error ratio, so it is one of the most important properties for an information carrier. Containing such a high extinction ratio, the encoding convertor is favorable for quantum communication. It is worth noting that, due to the asymmetry of the groove arrays in the y-direction, the maximum probabilities of SPPs coupled to different waveguides are different, so are the extinction ratios, which do not affect the conversion function of the encoding convertor.

Since the encoding convertor works on the interference of SPPs from different grooves, it has a limited working frequency band depending on the geometry of the encoding convertor. In spite of that, the encoding convertor with elaborate design can work over a broad spectral range in the visible frequency as shown in Fig. 3, where the conversion efficiency of the designed convertor is given as a function of frequency (400–530 THz). The conversion efficiency reaches 6.6% at 447 THz with a full width of half maximum (FWHM) of 30 THz (45 nm in vacuum wavelength). Since the properties of SPP depend on the material and geometry structure, the best working frequency can be manipulated by engineering the structure of the encoding convertor as required, which increases its feasibility. What is more, the two probabilities exhibit the same profile, which means that they have the same working frequency band for the conversion from $|+\rangle$ to right route (black line) and $|-\rangle$ to left route (red line). In the inset of Fig. 3, the corresponding extinction ratios are also given, which agrees well with the conversion efficiency in the working frequency band. Both conversion efficiency and extinction ratio promise a broad bandwidth, and the customizable best working frequency makes the encoding convertor feasible and welcome in PICs.

In conclusion, a method to convert spin encoding to route encoding is proposed based on the polarization-dependent excitation of SPP. The designed encoding convertor can couple photons in different spin states to SPPs propagating in different routes with a conversion efficiency up to 6.6% at 447 THz and a FWHM of 30 THz. The extinction ratio of the encoding convertor reaches 93:1, which helps to reduce the bit error ratio and im-

prove the fidelity of the transmitted information in quantum communication. Besides, the broad bandwidth and customizable best working frequency expand the application scope of the encoding convertor. In addition, the development of PICs and free-space optics, which calls for a connection between spin encoding and route encoding, makes the encoding convertor important in exchanging information. This friendly way built between spin encoding and route encoding improves the compatibility of spatial optics and integrated optics, and the encoding convertor will play an important role in the quantum communication.

References

1. T. W. Ebbesen, H. J. Lezec, H. F. Ghaemi, T. Thio, and P. A. Wolff, Nature **391,** 0028 (1998)
2. E. Altewischer, M. P. van Exter, and J. P. Woerdman, Nature **418,** 304 (2002).
3. X.-F. Ren, G.-P. Guo, Y.-F. Huang, C.-F. Li, and G.-C. Guo, Euro. Phys. Lett. **76,** 753 (2006).
4. Y. Gorodetski, N. Shitrit, I. Bretner, V. Kleiner, and E. Hasman, Nano Lett. **9,** 3016 (2009).
5. K. V. Nerkararyan, Phys. Lett. A **237,** 103 (1997).
6. E. Ozbay, Science **311,** 189 (2006).
7. H. A. Atwater and A. Polman, Nature Mater. **9,** 205 (2010).
8. A.-P. Liu, X. Xiong, X.-F. Ren, Y.-J. Cai, G.-H. Rui, Q.-W. Zhan, G.-C. Guo, and G.-P. Guo, Sci. Rep. **3,** 2402 (2013).
9. J. Zhou, J. Zhang, C. Wang, Z. Zhao, J. He, X. Tao, and X. Luo, Chin. Opt. Lett. **11,** S22401 (2013).
10. E. Prodan, C. Radloff, N. J. Halas, and P. Nordlander, Science **302,** 419 (2003).
11. A. Crespi, R. Ramponi, R. Osellame, L. Sansoni, I. Bongioanni, F. Sciarrino, G. Vallone, and P. Mataloni, Nature Commun. **2,** 566 (2011).
12. J. Takahara, S. Yamagishi, H. Taki, A. Morimoto, and T. Kobayashi, Opt. Lett. **22,** 475 (1997).
13. G. N. M. Tabia, Phys. Rev. A **86,** 062107 (2012).
14. Z. Chen, J. Chen, Y. Li, J. Qian, J. Qi, J. Xu, and Q. Sun, Chin. Opt. Lett. **11,** 112401 (2013).
15. R. D. Roy, R. Chattopadhyay, and S. K. Bhadra, Photon. Res. **1,** 164 (2013).
16. J. Lin, J. P. B. Mueller, Q. Wang, G. Yuan, N. Antoniou, X.-C. Yuan, and F. Capasso, Science **340,** 331 (2013).
17. E. D. Palik, *Handbook of Optical Constants of Solids* (Academic, 1998).
18. N. Yu, P. Genevet, M. A. Kats, F. Aieta, J.-P. Tetienne, F. Capasso, and Z. Gaburro, Science **334,** 333 (2011).